

Investigations on the total radiation efficiency of ribbed plates floating on water

Xia Pan, Ian MacGillivray, Vinh Trinh and James Forrest

Maritime Division, Defence Science and Technology Group, Victoria, Australia

ABSTRACT

The total radiation efficiency of ribbed plates floating on water is often used as a basis on which to represent the sound radiation from ribbed stiffened ship hulls. Investigations of this efficiency of plates are presented in this paper. Two numerical plate models are developed using the finite element programs ANSYS and Actran and compared with an approximate analytical model. Results of experiments conducted in a water tank are compared with the numerical and analytical methods. Good agreement is obtained from all the methods up to 10 kHz. Above 10 kHz Actran and experimental results were not available, but both the ANSYS and the analytical methods agree well until just below the plate critical frequency of about 78 kHz. Above the critical frequency, no comparison is carried out. The results shown provide confidence in the above methods to conduct detailed studies of complex structures, such as ship hulls.

1 INTRODUCTION

In naval applications, it is important to be able to estimate the noise radiated underwater by a vibrating hull structure during its design stage. The radiation efficiency of a ribbed plate floating on water may be used as a benchmark to represent the sound radiation from the hull of a surface vessel.

Analytical and numerical methods are both important in the analysis of structure-borne noise. For simple structures, analytical solutions can be obtained and the mechanism of vibration and noise production can be analyzed in detail. For complex structures, numerical finite element (FE) and/or boundary element (BE) methods can be used to model vibration and noise radiation, which has made them a popular choice in recent years. However, the computing times of the numerical methods increase rapidly – and instability problems may occur – as the frequency increases.

In a classic paper, Maidanik (1962) empirically developed an analytical method for the radiation efficiency of ribbed plates. He proposed approximate formulae for the efficiency in different frequency ranges of a simply supported plate in an acoustic baffle in air. Leppington et al. (1982) provided a detailed mathematical analysis of the radiation from modes of a simply supported panel including the multi-modal case. Their results mostly agreed with the formulae of Maidanik (1962) but they proposed a modified result close to the critical frequency. Oppenheimer and Dubowsky (1997) developed Maidanik's method to calculate an approximate efficiency of a plate without a baffle for frequencies below the plate critical frequency. They presented a corrected efficiency containing scaling factors whose values were chosen empirically by comparison with measured data. More recently, Putra and Thompson (2010) extended Maidanik's method for a baffled plate in air to the case of an unbaffled plate in air using an empirical formula. They showed the difference in the efficiency between the baffled and unbaffled plates. The large effect at low frequencies is caused by the change from a monopole to dipole characteristic. Removal of the baffle is shown to lead to a significant reduction of radiation efficiency in the corner and edge mode regions.

Cheng et al. (2012) provided an analytical model for a baffled plate in water. Pan et al. (2016) developed two numerical FE / BE models to evaluate the efficiency of an unbaffled flat plate totally submerged in water. They also presented an approximate analytical model. Good agreement was obtained between the numerical and analytical results.

As it is difficult to measure the efficiency in water, most published experimental results have been for a plate in air (Maidanik 1962, Fahy 1985, Oppenheimer and Dubowsky 1997 and Putra et al. 2014), usually with an "infinite" (i.e. large) rigid baffle. Zhao et al. (2012) measured sound radiation of submerged stiffened plates in a lake to compare to a statistical energy analysis (SEA) calculation. They modified the SEA method of averaging the radiation efficiency in air to that in water. The comparison of the modified SEA results with their measured data gave satisfactory agreement. However, the surface velocity of the plate and the radiated sound power were not measured simultaneously.

The aim of the work described in this paper is to investigate analytical, numerical and experimental capabilities and limitations to estimate the underwater noise radiation. Two numerical FE models are developed to evaluate the radiation efficiency of a floating ribbed plate. An approximate analytical model is also presented. To validate the analytical and numerical models, experiments were performed. The experiments were conducted in a water tank where surface velocity and radiated sound power were measured simultaneously. The results of the experiments are compared with the analytical and numerical results for two floating ribbed plates.

2 THEORETICAL METHOD

The relation of radiation efficiency and radiated sound power given by Oppenheimer and Dubowsky (1997) is

$$\sigma = \frac{W_r}{\rho c S \langle \bar{V}^2 \rangle} \quad (1)$$

where W_r is the radiated sound power from one side of the plate if baffled or both sides of the plate if unbaffled, ρ is the density of the fluid, c is the speed of sound in the fluid, S is the plate radiating surface area and $\langle \bar{V}^2 \rangle$ is the spatially averaged mean-square normal velocity of the plate.

2.1 Radiation efficiency of a ribbed plate in an acoustic baffle in air

The total radiation efficiency for frequencies below the plate critical frequency has been previously presented by averaging radiation efficiencies of the modes of a simply supported baffled plate (Maidanik 1962). The total efficiency of a simply supported baffled flat plate in air was expressed by Oppenheimer and Dubowsky (1997) as

$$\sigma_{baf} = \sigma_{corner} + \sigma_{edge}, \quad f < f_c \quad (2)$$

where σ_{corner} and σ_{edge} are the modal average radiation efficiencies for the corner and edge modes, and f_c is the critical frequency of the plate, which can be estimated by (Bies and Hansen 1997)

$$f_c = \frac{0.55c^2}{c_L h} = \frac{0.55c^2}{h \sqrt{E/\rho_s(1-\nu^2)}} \quad (3)$$

where h is the thickness of the plate and c_L is the speed of longitudinal waves in the plate, which can be expressed as shown in terms of the Young's modulus E , material density ρ_s and Poisson's ratio ν of the plate. For a simply supported baffled flat plate in air, an approximation for σ_{corner} and σ_{edge} were given by Maidanik (1962).

If the plate has ribs, Maidanik (1962) concluded that ribbing would increase the radiation efficiency of a plate below the critical frequency by a factor equal to

$$K^{ribs} = (P_r^{ribs} + P_r^0) / P_r^0, \quad (4)$$

where P_r^{ribs} is twice the total length of the ribs and P_r^0 is the perimeter of the original plate.

2.2 Radiation efficiency of a ribbed plate without an acoustic baffle in air

As a starting point, consider the total radiation efficiency for an unbaffled flat plate, originally given by Oppenheimer and Dubowsky (1997) as

$$\sigma_{unb} = F_{plate} (F_{corner} \sigma_{corner} + F_{edge} \sigma_{edge}), \quad f < f_c. \quad (5)$$

F_{plate} is a plate correction that accounts for inertial flow interaction between both sides of the plate, with the greatest effect at low frequencies. F_{corner} and F_{edge} are local corrections which account for sound radiation from the corners and edges at higher frequencies. These corrections are shown below. The first correction factor is

$$F_{plate} = \frac{\beta^4 k^4 S^2}{48\pi^2 \left(1 + \frac{\beta^4 k^4 S^2}{48\pi^2}\right)} \quad (6)$$

where k is the acoustic wavenumber and β is the proportionality factor of the plate. Note that values of β can vary significantly with medium type and plate size. The remaining correction factors are

$$F_{corner} = 0.5 \frac{13f}{f_c \left(1 + 13 \frac{f}{f_c}\right)}, \quad F_{edge} = 0.5 \frac{49f}{f_c \left(1 + 49 \frac{f}{f_c}\right)}. \quad (7)$$

If the plate has ribs, the ribbing would increase the efficiency by the factor K^{ribs} (given by Equation (4)). The efficiency of Oppenheimer and Dubowsky (1997) for an unbaffled ribbed plate is

$$\sigma_{unb}^{ribs} = K^{ribs} \sigma_{unb}, \quad f < f_c. \quad (8)$$

2.3 Radiation efficiency of a ribbed plate floating on water without an acoustic baffle

An analytical method for a ribbed plate floating on water appears not to exist in the literature. Some justification is therefore required in order to apply the above theory to such a situation. Figure 1(a) shows a planar plate floating on water, Figure 1(b) replaces the air half-space with a vacuum and Figure 1(c) shows the plate totally submerged in water.

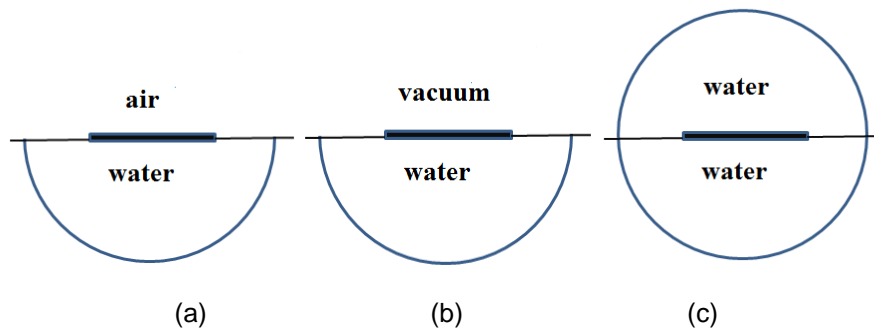


Figure 1: Modelling method for a plate: (a) floating on water; (b) air half-space assumed to be a vacuum; (c) totally submerged in water

The efficiencies in the three cases (a), (b) and (c) shown in Figure 1 are σ_a , σ_b and σ_c . Firstly, σ_a is almost identical to σ_b because the mass loading of the air is small relative to the water loading. Efficiency σ_b is due to sound power from one side of the plate (see Equation (1)). If the plate were to be replaced by a rigid piston, the radiation efficiencies of cases (b) and (c) would be identical by physical symmetry, with pressure zero on the baffled region in the plane of the plate. Note also that the sound power is double in case (c) but the radiating area is also doubled, so the efficiency is unaltered. For a non-rigid elastic plate, if the plate vibrations were the same in cases (b) and (c) it would therefore be expected that the radiation efficiencies would be similar. The additional added mass of case (c) reduces the magnitude of plate vibration, which in itself does not alter the radiation efficiency. However, it also lowers the modal frequencies of the plate, but not more than a factor of $\sqrt{2}$ depending upon the plate thickness, because of the doubling of added mass. The efficiency of the lowered modes is expected to be slightly less in case (c) accordingly, but only because of the lowered modal frequencies. Numerical simulations of case (a) and case (c) (not given here) have shown that σ_a is close to σ_c differ-

ing by about 3 dB over most frequencies of interest here, especially at low frequencies where the acoustic wavelengths are long. All efficiencies are therefore expected to be similar.

The radiation efficiency from the analytical method is based on Equations (1) to (8), where the density and sound speed of water are used. A single proportionality factor β in Equation (6) was chosen by comparison with experimental / numerical data and will be described in Section 5.

3 NUMERICAL METHODS

Two numerical models were developed for predicting the radiation efficiency of a floating plate. The first model is based on the FE method using the commercial software ANSYS. The second also used the FE method using the commercial software Actran. For the ANSYS method a harmonic point force with amplitude of 1 N perpendicular to the plate was applied to calculate the velocity distribution and sound power. For the Actran method it was easier to apply a fixed displacement amplitude normal to the plate at the same point. The total radiation efficiency was calculated by averaging the efficiencies due to three point positions as shown in Figure 2(a) for an edge ribbed plate and Figure 2(b) for an edge and surface ribbed plate. Note that the force (or displacement) locations are different on the two plates in order to match those in the experiments. In the case of the edge and surface ribbed plate, the forces are located on ribs.

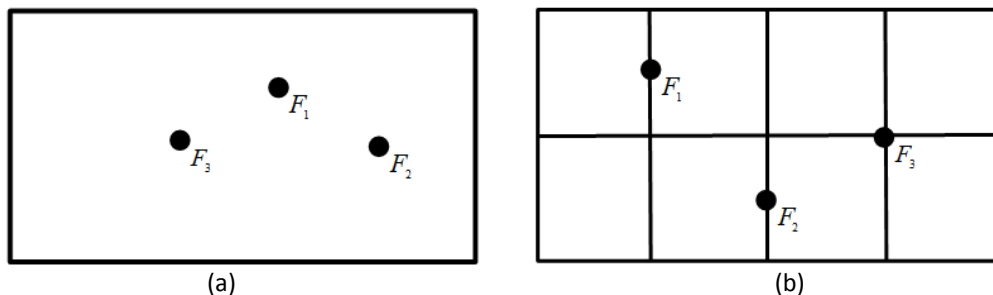


Figure 2: Top view of positions of point forces for a plate: (a) edge ribbed; (b) edge and surface ribbed

3.1 ANSYS method

For the first FE model, ANSYS Acoustics was used and a damping loss factor 0.02 was applied to the plate material. Figure 3 shows the ANSYS model of the plate structure used to calculate sound radiation. In order to calculate the radiation of structures floating on water (see Figure 1(a)), a fully coupled structural acoustic model was developed.

The fully coupled model consisted of the plate structure and acoustic bodies. The structure was floating on water with the middle plane of the base plate in the same plane as the air or water surface. The air surface was on the ribbed side of each plate. For each medium type (water or air) one acoustic body was created as a computational domain enclosing the plate structure on that side of the surface. The remaining acoustic body was the perfectly matched layer enclosing each computational domain with water or air depending on the domain. Figure 4 shows a plate, computational domain and perfectly matched layer of the section plane. All meshes of the plate structure and acoustic bodies were connected. The fully coupled analysis accounts for the fluid–structure interaction.

Due to the limitation of the computer memory to run the ANSYS models, the ANSYS results were obtained by averaging 3 points in each one-third band. The three points were chosen at the central frequency and two adjacent frequencies in each band. Convergence tests were carried out and showed that averaging three points was sufficient for the plate structure as structural damping was included in the ANSYS model.

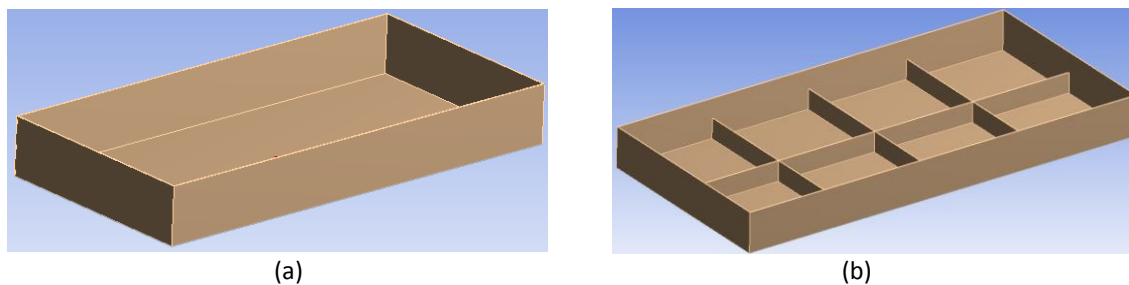


Figure 3: Plate structures using FE (ANSYS): (a) edge ribbed plate;
(b) edge and surface ribbed plate

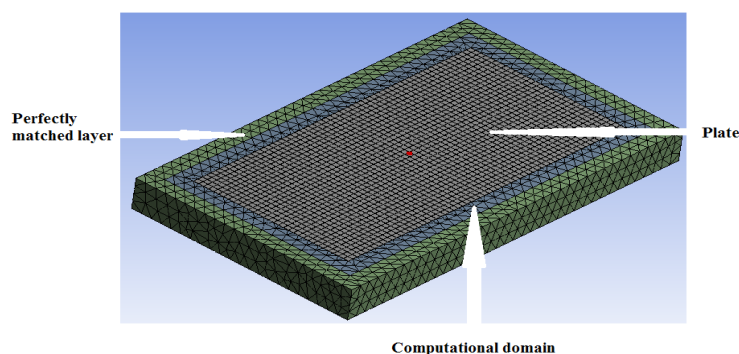


Figure 4: FE (ANSYS) model showing a plate, computational domain and perfectly matched layer on a section plane

3.2 Actran method

For the second FE model, the software Actran was used. No damping was used in the plate structures (apart from radiation) and, as the calculations are historical, they could not be repeated (no damping or increase in frequency range could be modelled). The models used matched those of Figure 3 for ANSYS, and full coupling was used between the plate and water. Calculations were performed using Actran's Krylov solver by subdividing the frequency range of interest into sub-regions, allowing the dynamic stiffness matrix to be approximated piecewise by polynomials for more rapid calculation. Six frequency regions over the range 50 Hz to 10000 Hz were found to be adequate. Before fractional-octave averaging, the actual frequency resolution ranged from 10 Hz at 50 Hz to 50 Hz at 10000 Hz. A soft baffle was used to model the water surface. An infinite domain was used to model the semi-infinite water half-space, and the air half-space was assumed to be a vacuum (see Figure 1(b)). As previously stated, displacement boundary conditions were used to excite the plates at the points shown in Figure 2.

4 EXPERIMENTAL METHOD

The experiments were conducted in a water tank of dimensions 6 m \times 6 m \times 4 m, in the Maritime Division at Defence Science and Technology Group. This water tank was constructed with steel and was built above ground so it can be regarded as a highly reverberant environment. An electrodynamic shaker was used to excite the plates with band-limited random noise to cover all one-third octave bands of interest. The shaker was isolated from the water tank. Three shaker locations were used, approximating those (F_1 , F_2 and F_3 locations) shown in Figure 2. The underwater radiation efficiency of the plates was evaluated using Equation (1). Twelve accelerometers were distributed randomly on the plate to obtain the mean-square surface velocity $\langle \bar{v}^2 \rangle$. Twenty hydrophones were also distributed randomly in the water tank to measure the sound pressure levels. The results were then averaged and the underwater sound power W_r of the plate was obtained using a reverberation time technique. The reverberation time of the water tank was measured separately using an adaptation of the reverberation time technique described by Jones and Hoefs (1996). The total efficiency was obtained by averaging the efficiencies due to the three shaker positions.

The radiation efficiencies were measured for both edge ribbed plate and edge and surface ribbed plate floating on water. The edge ribbed plate was measured first. The same plate then had internal ribs (stiffeners) added to it, to ensure that differences in results were mainly due to the introduction of the inner ribs, and the measurement was repeated for comparison. Figure 5 shows a test plate (edge and surface ribbed). Figure 6(a) shows the experimental set up, which simulates the case shown in Figure 1(a), and Figure 6(b) shows the instrumentation connection diagram. The experimental arrangement was used to determine simultaneously the surface velocity of the plate and the sound power radiated by the plate into the water.

The experimental results were measured from 1 kHz to 10 kHz. The 10 kHz limit is due to the upper frequency limit of the instrumentation system. The 1 kHz limit is due to the lower frequency limit of the water tank. Below 1 kHz, the modal density is too low for the reverberation time measurement to be accurate.



Figure 5: A test plate

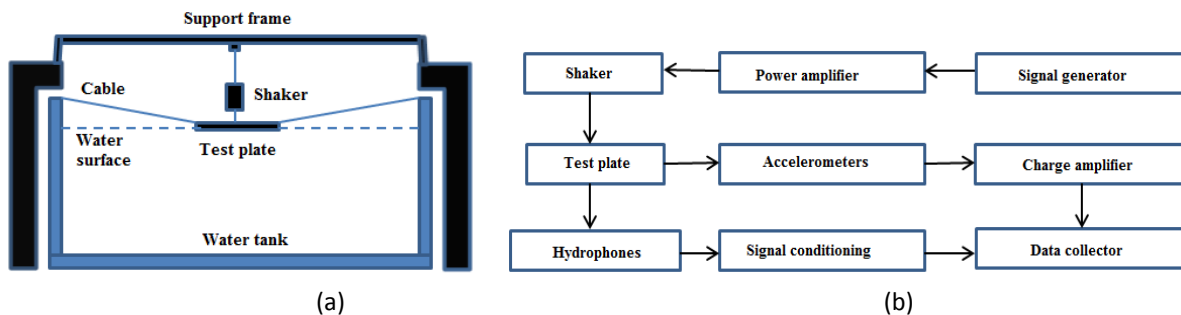


Figure 6: Experimental arrangement: (a) general set up; (b) instrumentation connection diagram

5 RESULTS

The analytical, numerical and experimental results presented here have been conducted for two steel plates, each with length 1.44 m, width 0.71 m and thickness 0.003 m. The edging ribs have height 0.2 m and the inside ribs have height 0.1 m. All ribs are 0.003 m thick. The critical frequency for all floating plates is approximately 78 kHz based on Equation (3) for a totally submerged plate.

For the analytical modelling, the proportionality factor $\beta = 0.7$ in Equation (6) was chosen empirically by comparison with the experiment / numerical data for all the plates. The value $\beta = 2$, originally used by Oppenheimer and Dubowsky (1997), was decreased to $\beta = 0.7$ to best fit the experimental / numerical data. For the ANSYS modelling, calculations were performed using different mesh resolutions in three frequency sub-divisions up to 75 kHz based on ANSYS Acoustics guidelines. For the Actran modelling typically 15000 elements were used. High-order 3D shell elements were used for the plate and the use of efficient infinite elements allowed the total number of elements to be kept low.

5.1 Edge ribbed Plate

Figures 7(a) to 7(c) show the comparisons of the radiation efficiencies of the edge ribbed plate due to three different force / displacement positions respectively (see Figure 2(a)). In Figure 7, the efficiencies plotted are the FE (ANSYS) data, the FE (Actran) narrow band data, the FE (Actran) averaged one-third octave band data and measured one-third octave band data. Note that the result obtained from the Actran model is only available for position 1 excitation. Good agreement is obtained from all the methods. There are some fine structures shown in Figure 7(a) for the Actran narrow band data. This structure is quite distinct because the Actran method did not include intrinsic plate damping.

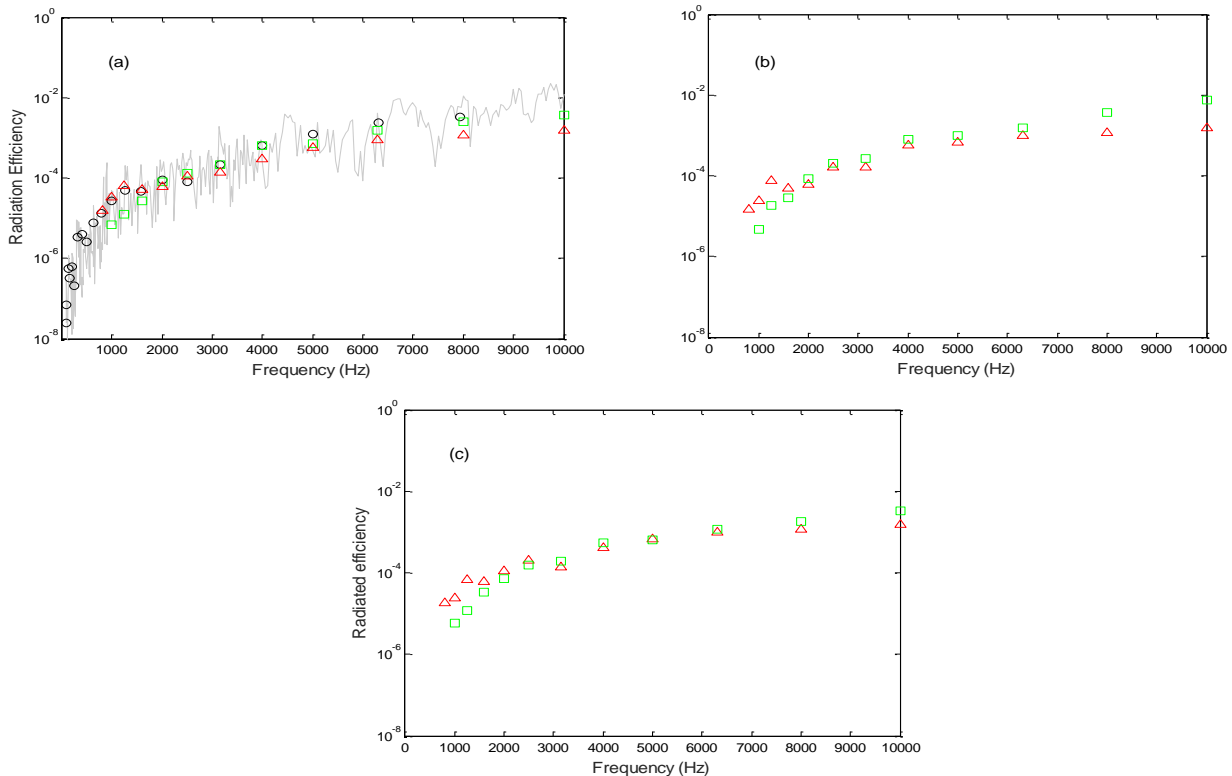


Figure 7: Radiation efficiency of the edge ribbed plate due to excitation at: (a) Position 1; (b) Position 2; (c) Position 3; $\Delta \Delta \Delta$, FE (ANSYS), —, FE (Actran) in narrow band, $\circ \circ \circ$, FE (Actran) averaged one-third octave band, $\square \square \square$, experiments

The total efficiencies from the numerical and experimental methods were obtained by averaging three force positions (see Figure 2(a)) and compared with analytical results (see Section 2). Figure 8 presents the comparison of the total efficiencies obtained from the analytical, numerical (ANSYS) and experimental methods. Results shown in Figure 8 demonstrate good agreement of the three methods except for frequencies between 1600 Hz to 3150 Hz. The difference may be due to the following reasons. Firstly, the ANSYS and experimental models are for the plate floating on water (see Figure 1(a) and Figure 6(a)); whereas the analytical model is for the plate totally submerged in water (see Figure 1(c)). Secondly, inadequate averaging is used. The analytical result is obtained as the average over all modes, while the numerical and experimental results are for three force excitation points which may not excite all modes. Thirdly, different boundary conditions (simply supported for the analytic model and ribbed edges for the numerical and the experimental models) are applied. Finally, experimental measurements have uncertainty and therefore error in measurements should not be disregarded.

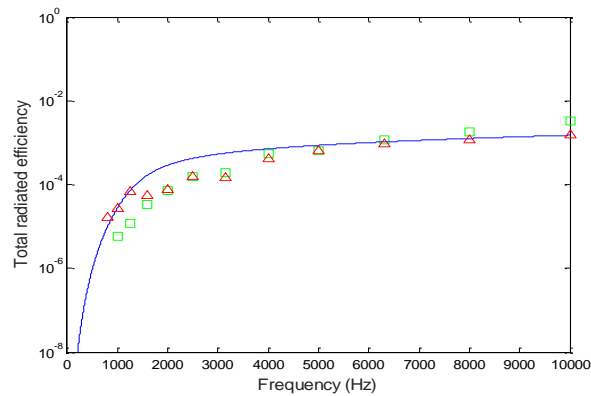


Figure 8: Total radiation efficiency of the edge ribbed plate. —, analytical method; $\Delta \Delta \Delta$, FE (ANSYS); $\square \square \square$, experiments

5.2 Edge and surface ribbed plate

Figures 9(a) to 9(c) show comparisons of radiation efficiencies of edge and surface ribbed plate due to the three different force positions (see Figure 2(b)). The agreement of all methods is shown to be satisfactory.

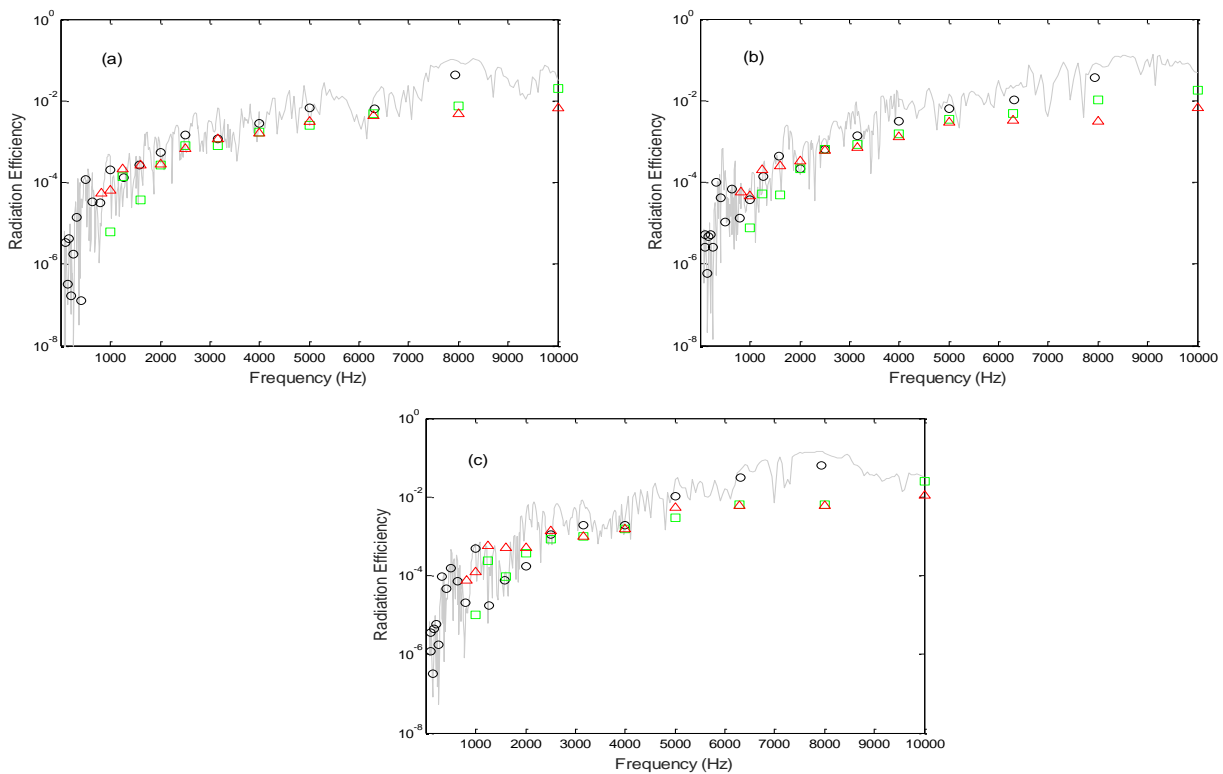


Figure 9: Radiation efficiency of the edge and surface ribbed plate due to excitation at: (a) Position 1; (b) Position 2; (c) Position 3. $\Delta \Delta \Delta$, FE (ANSYS), —, FE (Actran) in narrow band, $\circ \circ \circ$, FE (Actran) averaged one-third octave band, $\square \square \square$, experiments.

Figure 10 presents the comparison of the total efficiencies obtained from the analytical, the numerical (ANSYS / Actran) and the experimental methods. Results shown in Figure 10 demonstrate good agreement of all the methods at frequencies between 800 Hz and 6000 Hz. There are some differences at frequencies below 800 Hz and above 6000 Hz. Above 6000 Hz, the efficiency from the Actran method seems to be higher than those from other methods. This may be because the mesh in the Actran model could not be made fine enough at these frequencies. Other possible reasons for the differences are the same as those described in Section 5.1.

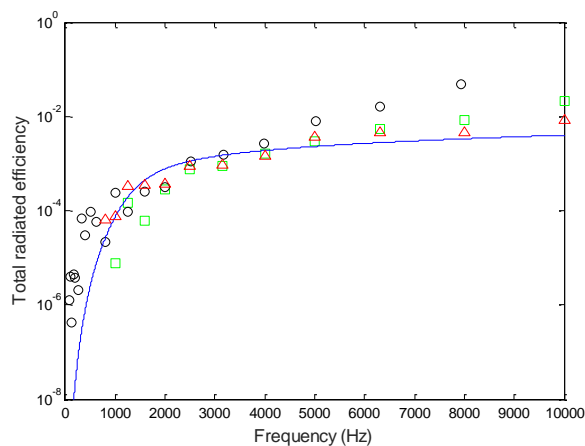


Figure 10: Total radiation efficiency of edge and surface ribbed plate. —, analytical method; $\Delta \Delta \Delta$, FE (ANSYS); $O O O$, FE (Actran); $\square \square \square$, experiments

5.3 Frequencies extended up to 75 kHz

In this section, the modelling frequency range is extended up to 75 kHz in order to view the efficiency just below the critical frequency of about 78 kHz. Only the analytical and the ANSYS models were used to obtain the following results as Actran and experimental results were not available above 10 kHz.

Figure 11 shows the comparison of the radiation efficiencies of the edge ribbed plate and edge and surface ribbed plate obtained from the analytical and the ANSYS models. Results predict that the ribbing increases the efficiency by about 5 dB. This is because stiff ribs effectively add more constraints to the plate, which can generate sound radiation below the critical frequency. The analytical results agree well with the ANSYS results below 70 kHz.

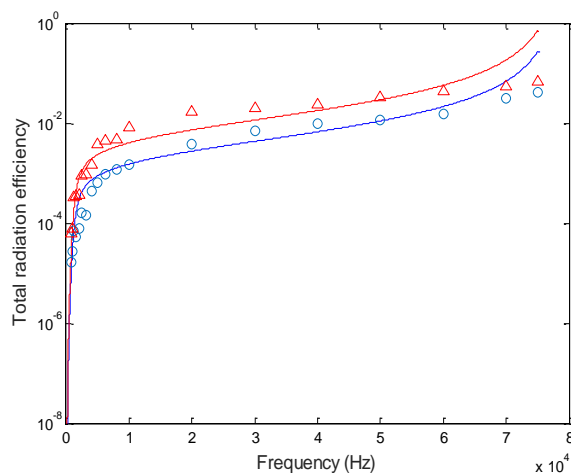


Figure 11: Total radiation efficiency of all plates using analytical method or FE (ANSYS):
 —, edge ribbed plate (analytical); $O O O$, edge ribbed plate (FE);
 —, edge and surface ribbed plate (analytical); $\Delta \Delta \Delta$, edge and surface ribbed plate (FE)

6 CONCLUSIONS

In order to develop a capability for predicting underwater noise radiation, several methods for estimating radiation efficiency have been investigated. Two numerical finite element models (ANSYS and Actran) have been developed to calculate the total radiation efficiency of ribbed plates floating on water below the critical frequency. As an analytical model for unbaffled ribbed plates floating on water has not been found in the literature, an approximate analytical model has been presented. The MATLAB code for the analytical model typically takes only 10 seconds for a solution. To validate the numerical and analytical models, experimental measurements

were conducted in a large reverberant water tank. The numerical and analytical results have been compared with measured data.

The effect of rib inclusion on the total efficiency was investigated. It was found that the ribbing increases the radiation efficiency of the test plates by about 5 dB. This is because stiff ribs effectively add more constraints to the plates, which can generate sound radiation below the critical frequency.

Good agreement has been obtained from all the methods up to 10 kHz. Above 10 kHz Actran and experimental results were not available, but both the ANSYS and the analytical methods agree well until just below the plate critical frequency of about 78 kHz. Above the critical frequency, no comparison has been carried out. The good agreement indicates the feasibility of using the above methods to conduct detailed studies of complex structures, such as ship hulls.

REFERENCES

- Bies, D.A. and Hansen, C.H. 1997, *Engineering Noise Control: Theory and Practice*, 2nd edition, London: Spon Press.
- Cheng, Z., Fan, J., Wang, B. and Tang, W. 2012, 'Radiation efficiency of submerged rectangular plates', *Applied Acoustics*, **73**, pp. 150-157.
- Cheng, Z., Fan, J., Wang, B. and Tang, W. 2012, 'Statistical analysis of vibration and sound radiation of submerged rectangular plates', *Science China: Technological Sciences*, **55**, pp. 3153-62.
- Fahy, F. 1985 *Sound and Structural Vibration: Radiation, Transmission and Response*, London: Academic Press.
- Jones, A.D. and Hoefs, S.A. 1996, 'Acoustical properties of the MOD Salisbury test tank and techniques for measurements', Report No. DSTO-RR-0068, Defence Science and Technology Organisation, Australia.
- Leppington, F.G., Broadbent, E.G., and Heron, K.H. 1982, 'The acoustic radiation efficiency of rectangular panels', *Proceedings Royal Society, London, Series A* **382**, pp. 245-27.
- Maidanik, G. 1962, 'Response of ribbed panels to reverberant acoustic fields', *Journal of the Acoustical Society of America*, **34**, pp. 809-826.
- Oppenheimer, C.H. and Dubowsky, S. 1997, 'A radiation efficiency for unbaffled plates with experimental validation', *Journal of Sound and Vibration*, **199**, pp. 473-489.
- Pan, X., MacGillivray, I. and Forrest, J. 2016, 'The effect of boundary conditions and ribs on the total radiation efficiency of submerged plates', *Proceedings of ACUSTICS 2016*, Brisbane, Australia.
- Putra, A. and Thompson, D.J. 2010, 'Sound radiation from rectangular baffled and unbaffled plates', *Applied Acoustics*, **71**, pp. 1113-1125.
- Putra, A., Shyafina N., Thompson, D., Muhammad, N., Jailani M., Nor, M. and Nuawi, Z. 2014, 'Modelling sound radiation from a baffled vibrating plate for different boundary conditions using an elementary source technique', *Proceedings of Inter-noise 2014*, Melbourne, Australia.